Advances in Concrete Construction, *Vol. 8, No. 2 (2019) 91-100*
DOI: https://doi.org/10.12989/acc.2019.8.2.091

Behavior of repaired RAC beam-column joints using steel welded wire mesh jacketed with cement mortar

Comingstarful Marthong*

Department of Civil Engineering, National Institute of Technology Meghalaya, Shillong 793003, India

(*Received July 23, 2018, Revised February 21, 2019, Accepted March 30, 2019*)

Abstract. In this paper three damaged exterior RC beam-column joints made of recycled aggregate concrete (RAC) were repaired. The aim of the study was to restore back the lost capacity of the beam-column joint to the original state or more. A relatively cheap material locally available galvanized steel welded wire mesh (GSWWM) of grid size 25 mm was used to confine the damaged region and then jacketed with cement mortar. Repaired specimens were also subjected to similar cyclic displacement as those of unrepaired specimens. Seismic parameters such as load carrying capacity, ductility, energy dissipation, stiffness degradation etc. were analyzed. Results show that repaired specimens exhibited better seismic performance and hence the adopted repairing strategies could be considered as satisfactory. These findings would be helpful to the field engineers to adopt a suitable rapid and cost efficient repairing technique for restoring the damaged frame structural joints for post earthquake usage.

Keywords: beam-column joint; recycled aggregate concrete; cyclic loading; repair; galvanized welded steel welded wire mesh; seismic performance

1. Introduction

As shown in Fig. 1, beam-column joints may be classified into three types viz. exterior joint, interior joint and corner joint. The behavior of these reinforced concrete (RC) beam-column joints plays an important role in the response of a framed structure. The key to the design of ductile moment-resisting frames is that the beam-to-column connections and columns must remain essentially elastic throughout the load history to insure the lateral stability of the structure (Tsonos 2007). In the past, numerous reinforced concrete frame structures collapsed due to severe earthquake. Post earthquake investigations into damaged structures generally showed that in many cases, damages of RC frame structure were localized in beam-column joint which might have led to partial or total collapse of the building. Further, it was observed that the exterior joints had suffered more in comparison to the interior ones.

Recycled aggregate has been use as a replacement of the natural aggregate (NA) for a number of years. Most of the past achievement on using recycled aggregate (RA) for concrete productions have been extensively reviewed and summarized by Behera *et al.* (2014). It shown that studies were mainly deal in the processing of demolished concrete, mixture design and characterizing the physical and mechanical properties (Shaikh *et al.* 2015, Subhash *et al.* 2016, Verma and Ashish 2017, Hamad *et al.* 2018). The mechanical and durability performances of recycled aggregate concrete (RAC) are generally inferior to

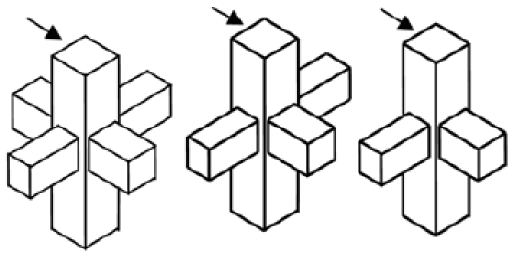

(a) Interior joint (b) Exterior joint (c) Corner joint

Fig. 1 Types of joints in a moment resisting frame

conventional concrete. This was perhaps the reason that RAC does not widely adopted in manufacturing structural elements. However, experimental investigations showed that reduction in mechanical strength is not much prominent, when RA replacement is up to 30% (Limbachiya *et al.* 2004, Rao *et al.* 2011, Xiao *et al.* 2012). Past studies concerning the behavior of beams (Han *et al.* 2001), columns (Chao *et al.* 2010) and beam-column joints (Corinaldesi and Moriconi 2006, Corinaldesi *et al*. 2011, Viviana *et al*. 2014, Marthong 2018), RC frame structure (Xiao *et al.* 2006) prepared from RAC are reported. Most of their findings on their structural behavior are positive, which reveal that cracking pattern and failure modes of the reinforced recycled aggregate concrete are quite similar to the conventional RC. After any major earthquake, there is always a concern about the effectiveness of a repairing technique which is also a cost effective, easy installation for repairing of damaged structures for post-earthquake usage. Therefore, to ensure further usability of the damaged structure effective repairing methodology needs to be investigated.

*Corresponding author, Associate Professor
E-mail: commarthong@nitm.ac.in

http://www.techno-press.org/?journal=acc&subpage=7
ISSN: 2287-5301 (Print), 2287-531X (Online)

2. Repairing methodology

The use of epoxy-bonded FRP sheets or strips as confining materials for repair or strengthening of RC beam-column joints has been reported by various researchers (Mosallam 2000, Ghobarah and said 2002, Mukherjee and Joshi 2005, Karayannis *et al.* 2008, Tsonos 2008, Saleh *et al.* 2010, Alsayed *et al.* 2010, Tsonos 2014, Hadi and Tran 2016, Ascione *et al.* 2017). Other method such as steel fiber ultra-high-strength concrete jackets without conventional reinforcement (Tsonos 2009, 2014) proved to be much more effective than the reinforced concrete jackets and the FRP-jackets when used for the earthquake-resistant strengthening of damaged reinforced concrete structural members. In all the mentioned studies, they showed that seismic capacity and failure modes of the RC beam-column joints significantly enhanced. However, in some studies anchoring of FRP materials has evolved as a difficult problem for the effectiveness of this technique (Ghobarah *et al.* 1997). Researchers also observed different types of failure that reduced the performance of FRP repaired structural elements (Esfahani *et al.* 2007, Teng *et al.* 2002). These failures are often brittle and include debonding of FRP. Thus, it is necessary to investigate an alternative material for FRP, which is more ductile and have better bond characteristic. In addition to FRP, stainless steel wire mesh composite (Choi 2008, Li *et al.* 2015, Kumar and Patel 2016, Patel *et al.* 2018), composite grid (Bentayeb *et al.* 2008) and geo-grid confinement (Chidambaran and Agarwal 2014) have also been investigated as strengthening methods to improve strength and ductility of RC structural elements. However, owing to the high manufacturing and application costs of these materials, the need has arisen to investigate other possible wrapping materials. Therefore, in this paper a relatively cheap materials i.e., galvanized steel welded wire mesh (GSWWM) locally available in the market was used to confine the damaged zone of RAC beam-column joint. The advantages of GSWWM are high tensile strength, rapid installation process and cost effective. Researchers (Corazao and Durrani 1989, FEMA 308 1998, Karayannis 1998, Marthong *et al.* 2013, Kalogeropoulos and Tsonos 2014, Shaaban and Seoud 2018) also observed that the effectiveness of any repairing or strengthening techniques depends on the treatment provided to the fragmented concrete in the damaged region. Hence, in this study an effort shall be focus on repairing the affected damage zone. Under higher damaged beam-column connections epoxy pressure injection of minor cracks and removal and replacement of the voids created is necessary for effective of any strengthening techniques (Tsonos and Papanikolaou 2003).

3. Experimental program

3.1 Selection of RC beam-column joints

An exterior isolated beam-column joint as shown in Fig. 2 was considered. It comprised of half the length of column on each side of the joint and part of the beam up to mid-span, which corresponded to the points of contra flexure in beam and column under lateral loads. The symmetric boundary conditions were maintained at both the ends of column for isolation of a single unit of beam-column joint. In this study, a typical full scale residential building with floor to floor height of 3.3 meters and the beam effective span of 3.0 meters were considered. The joint was scaled down to one-third size for experimental investigation.

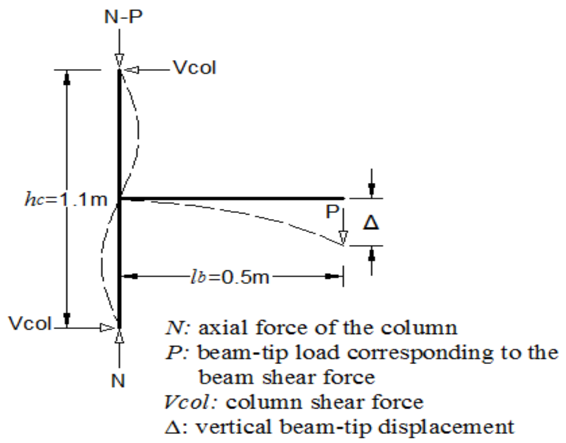

Fig. 2 Isolated exterior beam-column joint

3.2 Description and casting of RC beam-column joints

In the present study the three sets of exterior RC beam-column joints made of recycled aggregate concrete (RAC) which were previously damaged (Marthong 2018) were repaired. The joint types were (a) beam-column joint with beam weak in flexure (BWF) (b) beam-column joint with beam weak in shear (BWS) and (c) beam-column joint with column weak in shear (CWS). These specimens were made by replacing 30% of natural coarse aggregate (NCA) with recycled coarse aggregate (RCA) and were named as $BWF/_{RAC}$, $BWS/_{RAC}$ and $CWS/_{RAC}$ respectively. The repaired specimens were also compared to their respective control ones casted using an ordinary concrete of 100% of NCA (Marthong and Marthong 2016) i.e., $BWF/_{NAC}$, $BWS/_{NAC}$ and $CWS/_{NAC}$. Fig. 3 presented the reinforcement detailing of all specimens types. Longitudinal reinforcement consisted of high yield strength deformed (HYSD) bar of 8 mm diameter (Fe 500). Mild steel (MS) bar of 6 mm diameter (Fe 250) was also used as longitudinal as well as transverse reinforcement.

The detailing of BWF specimen is shown in Fig. 3(a). The cross section of column and beam is 100 mm×100 mm and 100 mm×120 mm respectively. Main bars consist of 8mm as well as 6mm diameter in both column and beam. A lateral tie of 6 mm diameter MS bar at 25 mm c/c spacing has been provided in the special confinement zone of the column, while the remaining part was increased to 50 mm c/c. The shear reinforcement provided in beam was of 6 mm diameter MS bar having spacing of 25 mm c/c near the beam-column joint for a length of 225 mm and a spacing of 40 mm c/c was provided in the remaining part.

Detailing of BWS specimens is shown in Fig. 3(b). The specimen in this category was similar in all respect to that

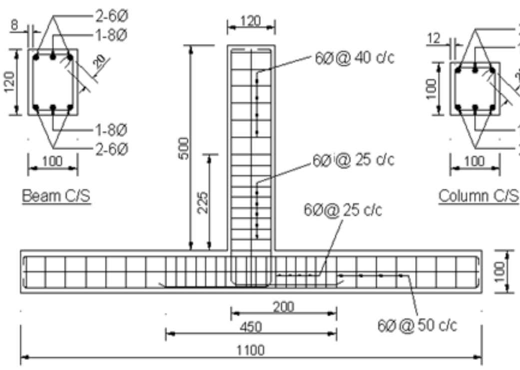

(a)

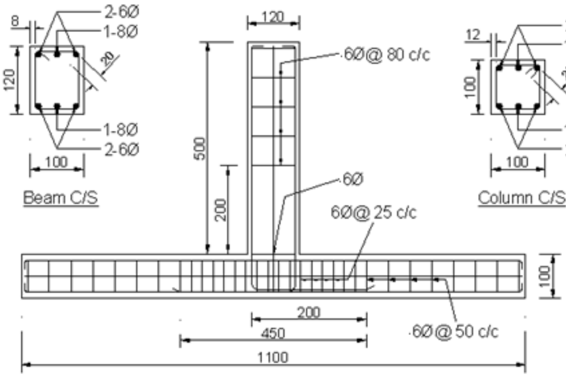

(b)

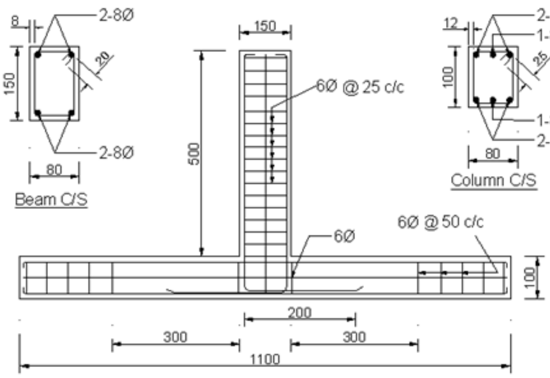

(c)

(All dimensions are in mm)

Fig. 3 Reinforcement detailing of specimens (a) BWF (b) BWS (c) CWS

of BWF specimen, except the shear reinforcement provided in beams. The amount of shear reinforcements has been reduced in order to make the beam weak in shear. In order to reduce the shear reinforcements in beam, lateral ties with 6 mm diameter bars with a spacing of 80 mm c/c were provided as shear reinforcement. To maintain the pre-defined failure location in the beam only the first two stirrups with a wider spacing of 200 mm c/c near the joint were placed.

The cross section of column as shown in Fig. 3(c) was kept same as that of BWF and BWS specimens, while the cross section of a beam was increased to 80 mm×150 mm. Main reinforcements in column were maintained similar to those of earlier cases, while same was increased in beam.

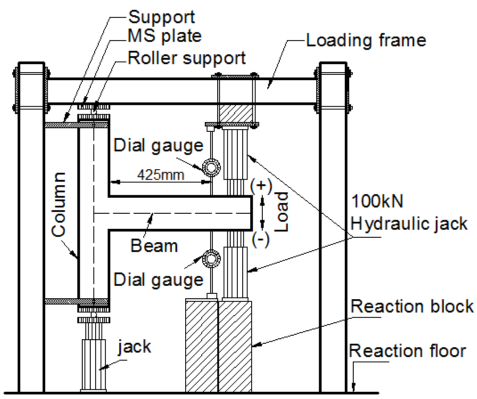

(a)

(b)

Fig. 4 Testing of beam-column joints (a) Test set-up (b) Actual testing arrangement

To ensure the shear weakness of these specimens a wider lateral ties spacing of 300 mm c/c on either side of the joint region has been provided. The spacing of lateral ties in the remaining part of column was reduced to 50 mm c/c. Table 1 presented the description of RC beam-column joints.

The concrete mix of all the beam-column joint specimens were designed for a characteristic cube compressive strength of 25 N/mm^2 which resulted in a target mean cube compressive strength of 31.6 N/mm^2 as per Indian code of practice (IS 10262-2009) and the compressive strength after 28 days was reported as 32.16 N/mm^2.

3.3 Test set-up and instrumentation

Schematic diagram of the test set-up and the actual testing arrangement is shown in Fig. 4. A loading frame of 500 kN capacity and hydraulic jack of 100 kN was used for applying the load to the specimens. In the testing frame, the column was placed in the vertical position while the beam was placed in horizontal position. An axial load using hydraulic jack was applied to the column to represent the gravity load. To model the actual conditions where the moments were approximately zero at the mid-span of the column when subjected to lateral loading a roller supports were provided at both ends of the column. The cyclic loading was applied manually at a distance of 100 mm from the free end of the beam by mean of two hydraulic jack mounted at top and at bottom. The hydraulic jack of 100 kN

Table 1 Descriptions of RC beam-column joints (Marthong 2018)

Specimen	Beam			Column		
	Span (mm)	Section (mm×mm)	Longitudinal Reinforcement	Length (mm)	Section (mm×mm)	Longitudinal Reinforcement
BWF & BWS[b]	500	100×120	1-8ϕ+2-6ϕ-top 1-8ϕ+2-6ϕ-bottom	1100	100×100	2-8ϕ+4-6ϕ
CWS	500	80×150	2-8ϕ-top 2- ϕ-bottom	1100	100×100	2-8ϕ+4-6ϕ

[b]Beam weak in shear specimens have same dimensions and longitudinal reinforcement as that of beam weak in flexure specimens except the shear reinforcement provided in beam.

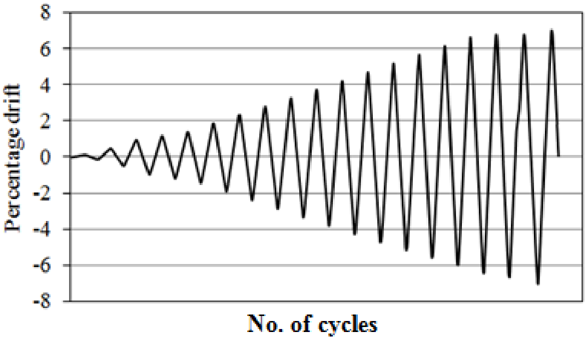

Fig. 5 Loading history

capacity was equipped with an in-built manually operated pumping units fitted with bourdon tube type load gauge and high pressure flexible hose pipe. Two dial gauges of 100 mm measuring range were placed at top and bottom face of the beam tip to measure the vertical displacement of the beam.

3.4 Loading sequence

The loading sequence suggested by Vidjeapriya and Jaya (2013) is adopted in the present study. However, one loading cycle at every amplitude of displacement was considered instead of three cycles. The loading history is presented in Fig. 5. A maximum displacement of ±30 mm was applied in all the specimens. The drift angle is defined as the ratio of beam tip displacement to the length of the beam measured from the joint to the position of the dial gauge. Drift obtained by horizontally displacing the beam ends are equivalent to the inter storey drift angle of a frame structure subjected to lateral loads. The two hydraulic jacks mounted on top and bottom of the beam tip end were used to apply the reversed cyclic loading. An axial load of 10% of gross capacity of column was applied to the column end by using a hydraulic jack to represent the dead load transferred from upper floors (Ghobarah *et al.* 1997).

3.5 Materials used for repairing

The repairing process involved removing of loose or fragmented concrete and then the void created were patched/filled back using micro-concrete (Renderoc RG) after a suitable bonding agent (Nitobond EP) was applied on the surface. The properties of micro-concrete and

Table 2 Properties of micro-concrete and bonding agent

Material	Properties	Value
Micro Concrete	Tensile strength	40 N/mm^2 @7 Days
	Tensile	2.0 N/mm^2 @7 Days
	Flexural strength	5.0 N/mm^2 @7 Days
Bonding agent	Compressive strength	50 N/mm^2 @7 Days
	Tensile strength	26 N/mm^2 @7 Days

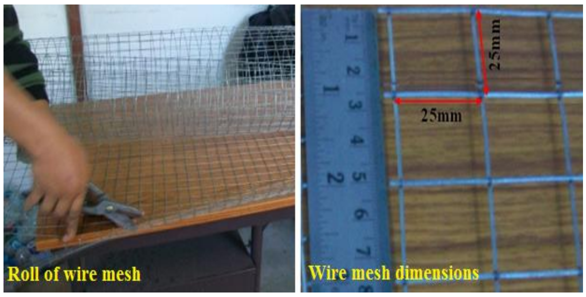

Fig. 6 GSWWM materials

bonding agent as obtained from the data sheet supplied by the manufacturer (Fosroc India Ltd.) are presented in Table 2. Locally available galvanized steel welded wire mesh (GSWWM) as shown in Fig. 6 was used to confine the damaged region. The opening of the mesh (grid size) was 25 mm square. The diameter of wires in the mesh was 1.2 mm. The yield strength of individual wires of the mesh was 300 MPa tested as per standard guidelines (ACI Committee 549 2008). The mix proportion of mortar jacketing was 1:2 by weight of cement and sand, respectively. The water to cement ratio was 0.45. The compressive strength of mortar cube was 20.23 N/mm^2 and 32.65 N/mm^2 at 7 and 28 days of curing respectively.

3.6 Rehabilitation strategies

The repairing consists of wrapping the damaged region of BWF/$_{RAC}$, BWS/$_{RAC}$ and CWS/$_{RAC}$ previously damaged (Marthong 2018) with two layers of GSWWM and jacketed with cement mortar. The repaired specimens were named as BWF/$_{Re}$, BWS/$_{Re}$ and CWS/$_{Re}$ respectively. Prior to wrapping with GSWWM the loose concrete on the damaged area is removed and the voids created after removal of loose materials were filled with micro-concrete after a suitable bonding agent was applied on the clean surface in order to attaining adequate bond between old and freshly added concrete. At 7 days of micro-concrete repairing the sharp corner of the joint region and partly on beam and column were rounded before placing of GSWWM. This is to facilitated stress reduction at the corners. Prior to wrapping with GSWWM a bonding agent was again applied on the hardened concrete surface for attaining adequate bonding between concrete and freshly applied mortar. After bonding agent has been applied approximately a 6 mm thick mix mortar of mixing ratio of 1:2 (cement: sand) by weight was placed on the surface of the specimens and then a wire mesh was wrapped around the joint and partly on beam and column depending on the extent of damage. Thereafter, the specimens were further plastered about 6 mm thick with the same mix mortar. All jacketed specimens were cured for 28

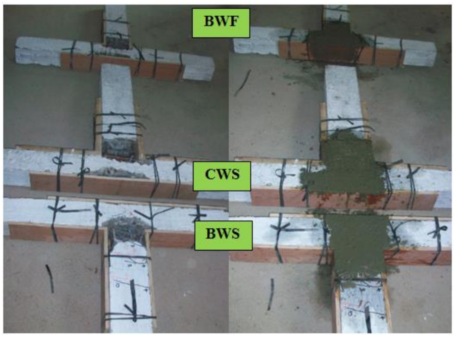

Fig. 7 Repair operations: Micro-concreting

Fig. 8 Repair operations: (a) Installation of GSWWM (b) and (c) GSWWM-mortar jacketing

Table 3 Strength and energy absorption of concrete specimens

Concrete Mix	Compressive strength (N/mm^2)	Tensile strength (N/mm^2)	Flexural strength (N/mm^2)
M-0	34.56	3.68	3.75
M-30	33.78	3.31	3.39

days from the date of jacketing and then were tested under a similar cyclic loading. Figs. 7 and 8 illustrates the repair operations.

4. Results and discussion

In the previous study (Marthong 2018) it was reported that 30% replacement of NCA with RCA reduces the workability (IS 1199 1959) of concrete by 15%. However, the same level of workability as those of mix with NCA could be achieved by adding superplastisizer of 0.5% by volume of water. The mechanical strength of test specimens is presented in Table 3. The results indicated a slight reduction in compressive strength (IS 519 1959) by 2%, tensile strength (IS 5816 1999) and flexural strength (IS 519 1959) by 10% at 30% replacement level. This reduction level may be considered acceptable (Hancen 1992, Limbachiya *et al.* 2004, Rao *et al.* 2011, Xiao *et al.* 2012).

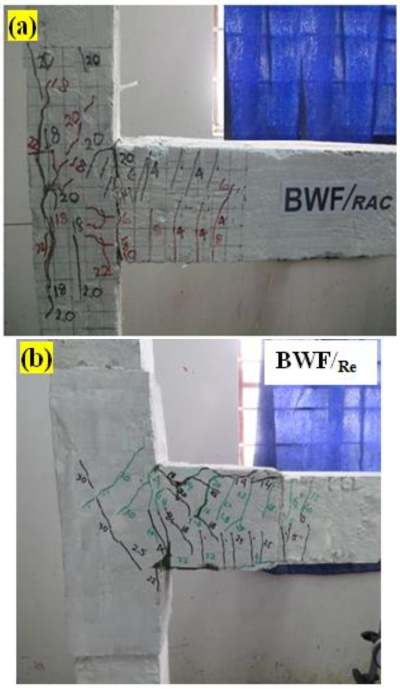

Fig. 9 Failure modes of BWF specimens

4.1 Failure mode of beam-column joints

Figs. 9, 10 and 11 presented the failure modes of beam-column joints due to cyclic loading. The initial cracks in all the beam-column joints mainly developed at the joint interface. On further application of cyclic loads, the cracks propagated toward their weakest shear zone or the flexural zone or widening up the initial cracks at the joint face and a maximum crack width of 5 mm was observed. It may be mentioned that all the control RAC specimens was taken from the previous studies (Marthong 2018). Observing the repaired BWF/$_{Re}$ specimen the flexural cracks is mainly concentrated in the beam part with only fewer crack propagated towards the joint region. The formation of a joint hinged was observed to delay for BWF/$_{Re}$ specimen as compared to the control specimens. This behaviour is due to the good bond characteristic provided by micro-concrete and GSWWM mortar jacketed.

It may be observed from Fig. 3(b) that the shear weakness in the beam for BWS specimens is over a length of 200 mm from the column interface. Examination of all the BWS specimens (Fig. 10) it show a visible shear cracks within the weak shear zone as expected. BWS/$_{RAC}$ (Marthong 2018) and BWS/$_{Re}$ specimens fail in a similar pattern with cracks not only concentrating on the weakest shear zone but also propagating towards the joint regions. A numbers of smaller cracks were distributed at the surface of the GSWWM jacketed at weakest shear zone and at the joint region for BWS/$_{Re}$, which improve the damage resistance under reversed cyclic loading compared to BWS/$_{RAC}$ specimen.

It may be also observed from Fig. 3(b) that the shear weakness in the beam for BWS specimens is over a length of 200 mm from the column interface. Examination of all the BWS specimens (Fig. 10) it show a visible shear cracks

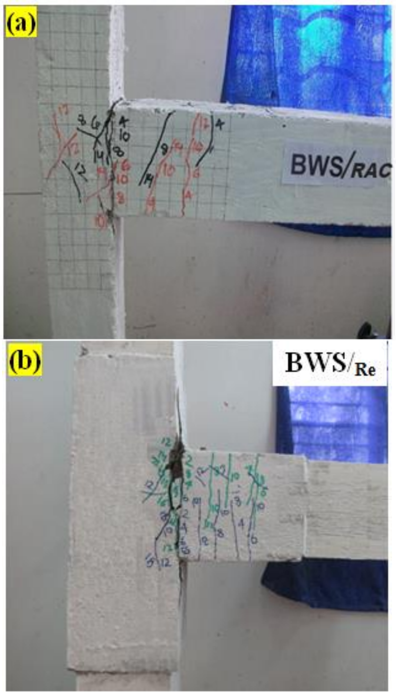

Fig. 10 Failure modes of BWS specimens

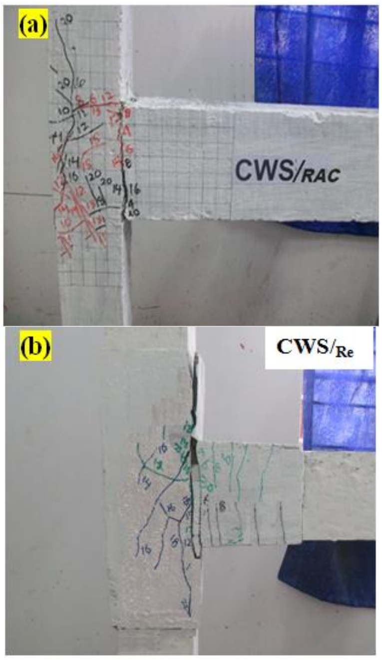

Fig. 11 Failure modes of CWS specimens

within the weak shear zone as expected. BWS/RAC (Marthong 2018) and BWS/Re specimens fail in a similar pattern with cracks not only concentrating on the weakest shear zone but also propagating towards the joint regions. A numbers of smaller cracks were distributed at the surface of the GSWWM jacketed at weakest shear zone and at the joint region for BWS/Re, which improve the damage resistance under reversed cyclic loading compared to BWS/RAC specimen.

Further, Fig. 11 presented the damage states of CWS specimens. Since the beam is much stronger than the

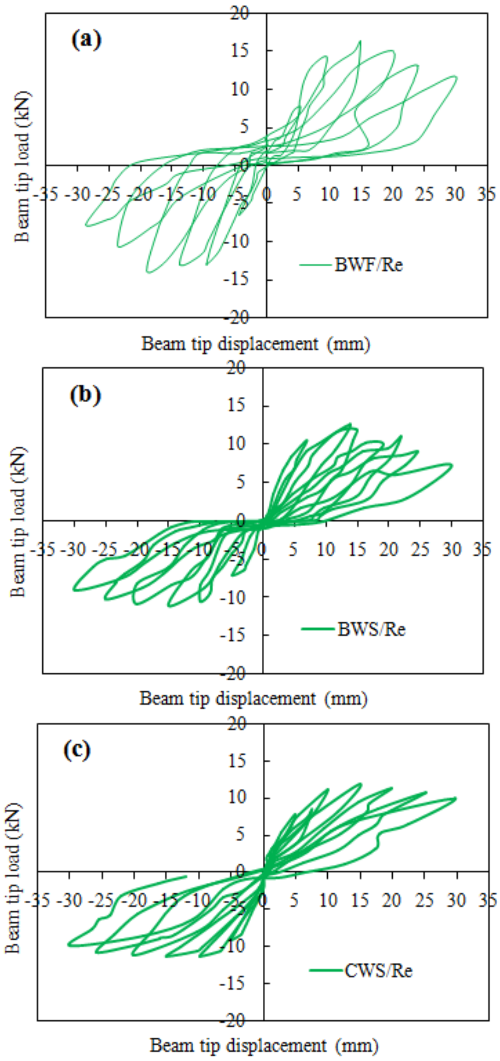

Fig. 12 Hysteretic responses (a) BWF (b) BWS and (c) CWS

column, cracks initiating from the joint region are propagating towards the weakest shear zone in the column, while the beam parts remain undamaged. The failure patterns of the specimens were as expected for CWS/RAC (Marthong 2018). However, confinement of the damaged joint region and partly in beam and column not only enhanced the load carrying capacity but also improved the failure pattern. As observed in Fig. 11(c) flexural failure also occurred in beam part with fewer crack in the joint region and column part as compared to CWS/RAC which is a desirable failure modes for stability of an RC frame.

4.2 Hysteretic response of specimens

The typical hysteretic response obtained by plotting the test data is presented in Fig. 12. Various seismic parameters such as ultimate strength, energy dissipation, stiffness degradations and ductility of the specimens were evaluated from these hysteretic responses. It may be mentioned that all the control specimens was taken from the previous studies (Marthong and Marthong 2016, Marthong 2018). Hence, for a better understanding of their performance the

Table 4 Capacity comparison of beam-column joints

Specimens	NAC (Marthong 2018 Marthong 2016) Average load capacity, (kN)	Energy dissipation (kN-mm)	Ductility (d_u/d_y)	RAC (Marthong 2018) Average load capacity, (kN)	Energy dissipation (kN-m)	Ductility (d_u/d_y)	Repair joints (present study) Average load capacity, (kN)	Energy dissipation (kN-m)	Ductility (d_u/d_y)
BWF	12.00	631.80	3.52	9.96	601.80	2.73	15.35	988.23	4.84
BWS	10.15	440.97	3.04	9.24	330.12	2.25	12.22	405.17	3.57
CWS	9.25	250.19	2.61	7.23	205.17	1.55	11.31	378.43	2.78

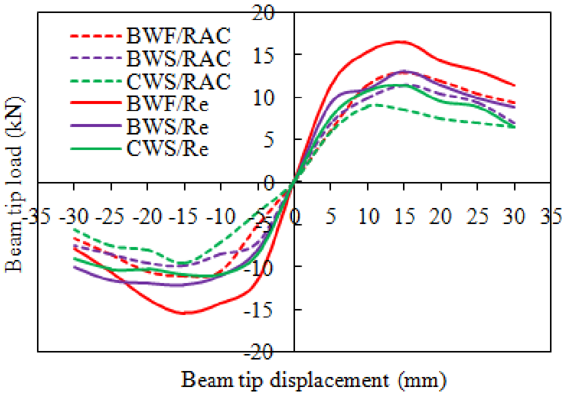

Fig. 13 Envelope curves

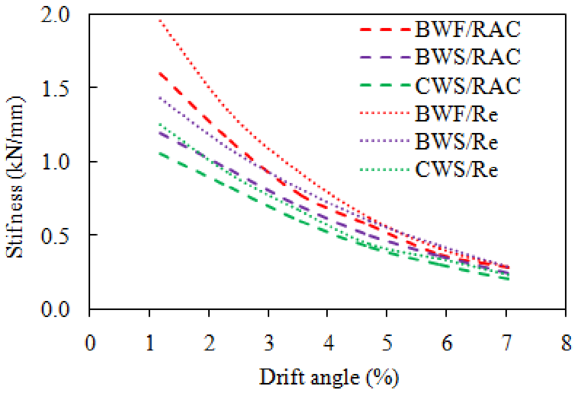

Fig. 14 Stiffness degradation

capacity comparison of the present study and previous tested similar specimens of both specimens prepared with natural aggregate concrete (NAC) and RAC is presented in Table 4. All the RAC specimens show decreases in load carrying capacity, energy dissipation and ductility while a significant increase of repaired joint was observed. The envelope curves as obtained from hysteresis loops are shown in Fig. 13. Comparing these curves of at each displacement, it can be observed that all repaired specimens show a similar load displacement characterization with the initial slope being relatively lower. The envelope of hysteresis loops of the repaired specimens, however, show higher load-carrying capacity in both push and pull directions for repaired specimens. Thus, all damaged RAC specimens could successfully restored the load-carrying capacity after repaired. This study shows that the appropriately chosen repair strategy could retrieve back the lost capacity of damaged structural component for post earthquake usage. Thus, it may be inferred that the applied repair techniques are effective in restoring the load-carrying capacity of the vital beam-column joints.

4.3 Stiffness degradation

Secant stiffness is evaluated as the peak-to-peak stiffness of the beam tip load-displacement relationship. The secant stiffness is an index of the response of the specimen during a cycle and its strength degradation from a cycle to the following cycle. It is calculated as the slope of the line joining the peak of positive and negative capacity at a given cycle. The slope of this straight line is the stiffness of the assemblage corresponding to that particular amplitude (Naeim and Kelly 1999). The typical stiffness degradation of the test specimens is presented in Fig. 14. Irrespective of the deficiency types, repaired specimens showed a similar degradation trend. Evaluating the reduction in stiffness of all the specimens it was observed that the degradation rate of stiffness is lower for repaired joints as compare to the corresponding control specimens at the same displacement level. The lower degradation of stiffness is a desirable property in earthquake like situations. It was observed during the past earthquake that most of the RC structures failed due to sudden loss of stiffness with increasing lateral movement. Therefore, from these comparisons it can be concluded that confinement of the damaged zone of RC beam-column joints using wire mesh lead to an enhancement of stiffness.

4.4 Cumulative energy dissipation

The performance of a structural element during seismic excitation depends to a large extent on its capacity to dissipate energy. The area of hysteresis loop is a measure of the energy dissipated. The cumulative energy dissipated at particular amplitude was calculated by summing up the energy dissipated in all the preceding cycles including that amplitude. The energy dissipation of specimens is presented in Table 4 and their variation with drift angle is presented in Fig. 15. As compared to their RAC specimens, the increased in energy dissipation is about 64%, 23% and 84% for BWF/$_{Re}$, BWS/$_{Re}$ and CWS/$_{Re}$ respectively, which is significant as compared to NAC specimens. The increase in stiffness at the end of imposed displacement history attracted more load corresponding to any drift angle due to high strength micro-concrete and mesh confinement, which prevent the initial crack propagations. Thus, the total area enclosed by the plot of beam tip load versus beam tip displacement was more. This was perhaps the reason for

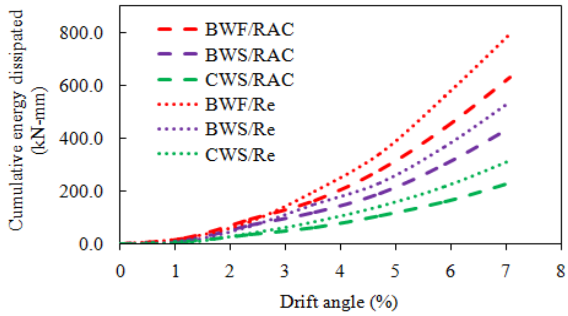

Fig. 15 Cumulative energy dissipation

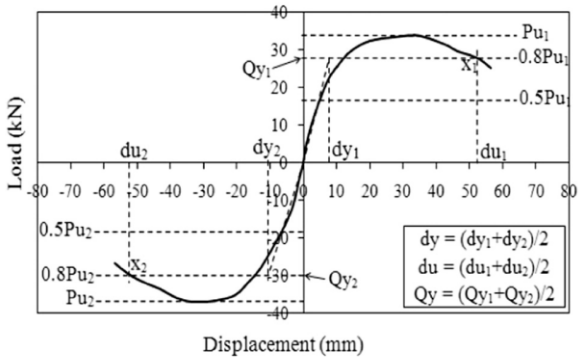

Fig. 16 Procedures for ductility calculation

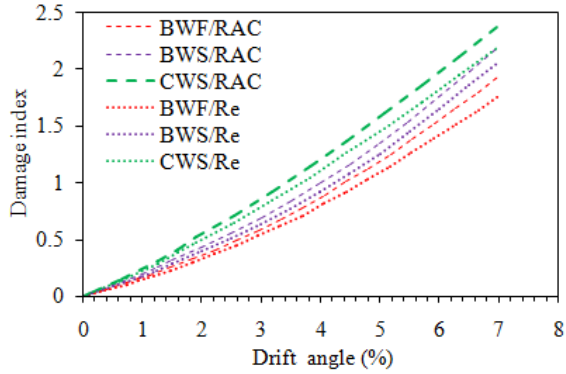

Fig. 17 Comparison of damage indices

improvement in cumulative energy dissipation in the subsequent loading cycles.

4.5 Displacement ductility

Displacement ductility is the ratio between the ultimate displacements (d_u) to the displacement at first yield (d_y) and was calculated from the load-displacement curve (Shannag *et al.* 2005). The procedure is explained in Fig. 16. The ultimate displacement (d_u) was set at a displacement corresponding to 20% drop of peak load for computation. The yield displacement is calculated as the point of intersection between two straight lines drawn in the envelope curve. The first line is obtained by extending the line joining the origin and 50% of ultimate load capacity point on positive and negative sides of the envelope curve, while the second line is obtained by drawing a horizontal line through the 80% of ultimate load capacity point on either side. In the Fig. 16, dy_1 and dy_2 represent the yield displacement in positive and negative direction on the envelope curve respectively. The average value of yield displacement as obtained from both positive and negative direction is calculated. Horizontal lines drawn through the 80% of ultimate load capacity point on positive and negative side intersect the envelope curve at far end at points x_1 and x_2. The average of abscissa of these two points (denoted by du_1 and du_2 in Fig. 16) is taken as maximum displacement. The displacement ductility is calculated as the ratio of maximum displacement to the yield displacement and these values are presented in Table 4. Significant increases in ductility of the damaged joints due to confined GSWWM which confirm the effectiveness of the repairing strategy.

4.6 Seismic damage index

Damage index model (Park and Ang (1985) given in Eq. (1) was employ in this study to evaluate the damage level of the specimens. The damage indices used as numerical indicators of damage of any structural element under any loading type. Parameters such as strain, displacement, strength, energy and intrinsic dynamic properties are used to calculate these damage indices.

$$DI = \frac{\delta_m}{\delta_u} + \frac{\beta}{\delta_u Q_y}\int dE \qquad (1)$$

where δ_m the maximum deflection attained during seismic loading, δ_u is the ultimate deflection capacity under monotonic load, $Q_y$is the yield force, dE is the incremental dissipated hysteretic energy and β is the strength degradation parameters. Parameters involved in the evaluation of the damage index were estimated as suggested (Karayannis *et al.* 2008). The calculated damage indices for all specimens based on the above model are presented in Fig. 17. These figures show that the damage indices increase as the damage of specimens grow further with increased drift values. Further, all the curves of the damage indices are nearly linear, which suggest that the growth of damages in rehabilitated specimens is similar to the undamaged control specimens and the damage trends are stable. The lower damage index presented by rehabilitated indicated an effectiveness of the adopted rehabilitation strategy. Among the three type of mesh adopted, GSWM-1 suggested to be most promising in term of providing ductility to the RC beam-column joints.

4.7 Nominal principal tensile stresses

To have a better understanding of their behavior, nominal principal tensile stresses in beam-column joint region (damaged regions) were evaluated and compared in Fig. 18. From this figures it is can be deduced that the developed nominal principal tensile stresses of all control specimens are slightly lower than those of the rehabilitated specimens. However, the ability of high strength epoxy resin confined with wire mesh jacket prevents the early crack initiation and crack propagation during cyclic loading; all rehabilitated specimens marginally increased

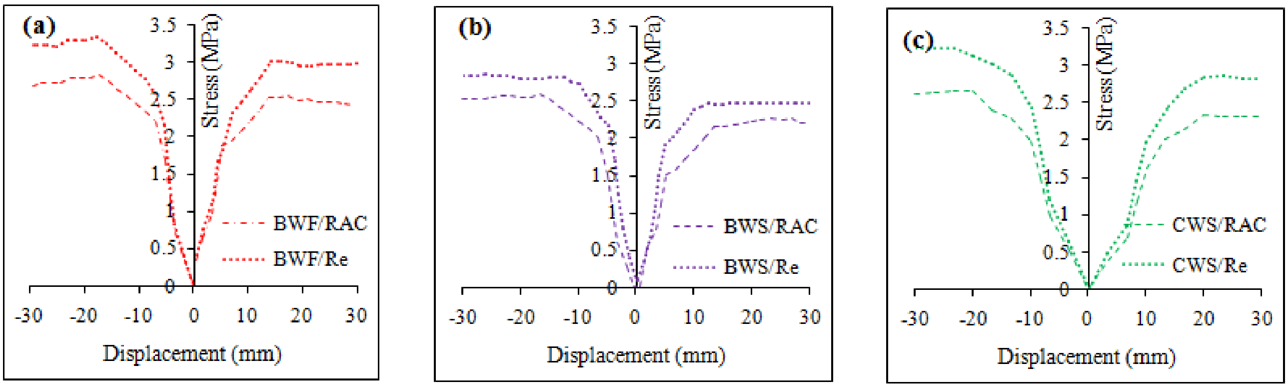

Fig. 18 Nominal principal tensile stress developed in beam

the nominal principal tensile stresses of the damaged specimens. This shows the effectiveness of rehabilitation technique to restore the tensile stress of the damaged joints to the original state or even higher.

5. Conclusions

The loose concrete in the damaged zone of exterior RAC beam-column joints were repaired using micro-concrete and then confined with galvanized steel welded wire mesh. Various parameters related to seismic capacity were evaluated and performances of these repaired specimens were evaluated by comparing its results with those obtained from the respective control specimens made with RAC and NAC. Based on experimental studies carried out, the following conclusions have been drawn.

• Comparison of important parameters related to seismic capacity such as ultimate load, stiffness degradation, energy dissipation, and ductility showed that the adopted repair strategies were satisfactory as damaged beam-column joints after repaired exhibited significant performances.

• Repaired specimens presented lower damage indices as compared to the corresponding un repair specimens

• Nominal principal tensile stresses of repaired substantially increased.

• Finally, the results of this study show that lost capacity of the damaged specimens could be retrieved back to the original state or more using a combination of micro-concrete and wire mesh jacketing at modest costs. The results suggest that wire mesh is the most efficient and economic material for increasing the seismic capacity.

References

ACI Committee 549 (2008), Thin Reinforced Cementitious Products & Ferrocement, American Concrete Institute, Farmington Hills, MI.

Alsayed, S.H., Al-Salloum, Y.A., Almusallam, T.H. and Siddiqui, N.A. (2010), "Seismic response of FRP-upgraded exterior RC beam-column joints", *J. Compos. Constr.*, ASCE, **14**(2), 195-208.

Ascione, F., Lamberti, M., Razaqpur, A.G. and Spadea, S. (2017), "Strength and stiffness of adhesively bonded GFRP beam-column moment resisting joints", *Compos. Struct.*, **60**, 1248-1257.

Behera, M., Bhattacharyya, S.K., Minocha, A.K., Deoliya, R. and Maiti, S. (2014), "Recycled aggregate from C&D waste & its use in concrete-A breakthrough towards sustainability in construction sector: A review", *Constr. Build. Mater.*, **68**, 501-516.

Bentayeb, F., Tahar, K.A. and Chateauneuf, A. (2008), "New technique for reinforcement of concrete columns confined by embedded composite grid", *Constr. Build. Mater.*, **22**, 1624-1633.

Chao, L., Guoliang, B., Letian, W. and Zonggang, Q. (2010), "Experimental study on the compression behavior of recycled concrete columns", *Proceedings of the International RILEM Conference on the Waste Engineering and Management*, 614-621.

Chidambaram, R.S. and Agarwal, P. (2014), "The confining effect of geo-grid on the mechanical properties of concrete specimens with steel fiber under compression and flexure", *Constr. Build. Mater.*, **71**, 628-637.

Choi, J.H. (2008), "Seismic retrofit of reinforced concrete circular columns using stainless steel wire mesh composite", *Can. J. Civil Eng.*, **35**(2), 140-147.

Corazao, M. and Durrani, A.J. (1989), "Repair and strengthening of beam-to-column joints subjected to earthquake loading", Technical Report NCEER-89-0013, National Center for Earthquake Engineering Research, State University of New York at Buffalo, N.Y.

Corinaldesi, V. and Moriconi, G. (2006), "Behavior of beam-column joints made of sustainable concrete under cyclic loading", *J. Mater. Civil Eng.*, **18**(5), 650-658.

Corinaldesi, V., Letelier, V. and Moriconi, G. (2011), "Behavior of beam-column joints made of recycled-aggregate concrete under cyclic loading", *Constr. Build. Mater.*, **2**, 1877-1882.

Esfahani, M.R., Kianoush, M.R. and Tajari, A.R. (2007), "Flexural behaviour of reinforced concrete beams strengthened by CFRP sheets", *Eng. Struct.*, **29**(10), 2428-2444.

Federal Emergency Management Agency (FEMA-308) (1998), Repair of Earthquake Damaged Concrete and Masonry Wall Buildings, 24-42.

Ghobarah, A. and Said, A. (2002), "Shear strengthening of beam-column joints", *Eng. Struct.*, **24**(7), 881-888.

Ghobarah, A., Aziz, A. and Biddah, T.S. (1997), "Rehabilitation of reinforced concrete frame joints using corrugated steel jacketing", *ACI Struct. J.*, **4**(3), 283-294.

Hadi, M.N.S. and Tran, T.M. (2016), "Seismic rehabilitation of reinforced concrete beam-column joints by bonding with concrete covers and wrapping with FRP composites", *Mater. Struct.*, **49**(1-2), 467-485.

Hamad, B.S., Daw, A.H., Daou, A. and Chehab, G.R. (2018), "Studies of the effect of recycled aggregates on flexural, shear, and bond splitting beam structural behavior", *Case Stud. Constr. Mater.*, **9**, e00186.

Han, B.C., Yun, H.D. and Chung, S.Y. (2001), "Shear capacity of reinforced concrete beams made with recycled aggregate", *ACI Spec. Publ.*, **200**, 503-516

Hansen, T.C. (1992), *Recycling of Demolished Concrete and Masonry*, Taylor and Francis, Oxfordshire, UK.

IS 10262 (2009), Guidelines for Concrete Mix Design Proportioning (CED 2: Cement and Concrete), Bureau of Indian Standard New Delhi.

IS 1199 (1959), Methods of Sampling and Analysis of Concrete, Bureau of Indian Standard New Delhi.

IS 519 (1959), Method of Tests for Strength of Concrete, Bureau of Indian Standard New Delhi.

IS 5816 (1999), Method of Test Splitting Tensile Strength, Bureau of Indian Standard New Delhi.

Kalogeropoulos, G.I. and Tsonos, A.G. (2014), "Effectiveness of R/C jacketing of substandard R/C columns with short lap splices", *Struct. Monit. Mainten.*, **1**(3), 273-292.

Karayannis, C.G. and Sirkelis, G.M. (2008), "Strengthening and rehabilitation of RC beam-column joints using C-FRP jacketing and epoxy resin injection", *J. Earthq. Eng. Struct. Dyn.*, **37**, 769-790.

Karayannis, C.G., Chalioris, C.E. and Sideris, K.K. (1998), "Effectiveness of RC beam-column joint repair using epoxy resin injections", *J. Earthq. Eng.*, **2**(2), 217-240.

Kumar, V. and Patel, P.V. (2016), "Strengthening of axially loaded circular concrete columns using stainless steel wire mesh (SSWM)-Experimental investigations", *Constr. Build. Mater.*, **124**, 186-198.

Li, B., Lam, E.S., Wu, B. and Wang, Y. (2015), "Seismic behavior of reinforced concrete exterior beam-column joints strengthened by ferrocement composites", *Earthq. Struct.*, **9**(1), 233-256.

Limbachiya, M.C., Koulouris, A., Roberts, J.J. and Fried, A.N. (2004), "Performance of recycled aggregate concrete", *RILEM International Symposium on Environment Conscious Materials and System for Sustainable Development*, 127-136.

Marthong, C. (2018), "Behaviour of recycled aggregate concrete beam-column connections in presence of PET fibers at the joint region", *Comput. Concrete*, **21**(6), 669-679.

Marthong, C. and Marthong, S. (2016), "An experimental study on the effect of PET fibers on the behavior of exterior RC beam-column connection subjected to reversed cyclic loading", *Struct.*, **5**, 175-185.

Marthong, C., Dutta, A. and Deb, S.K. (2013), "Seismic rehabilitation of RC exterior beam-column joints using epoxy resin injection", *J. Earthq. Eng.*, **17**(3), 378-398.

Mosallam, A.S. (2000), "Strength and ductility of reinforced concrete moment frame joints strengthened with quasi-Isotropic laminates", *Compos. Part B-Eng.*, **31**(6-7), 481-497.

Mukherjee, A. and Joshi, M. (2005), "FRPC reinforced concrete beam-column joints under cyclic excitation", *Compos. Struct.*, **70**, 185-199.

Naeim, F. and Kelly, J.M. (1999), *Design of Seismic Isolated Structures from Theory to Practice*, John willey & sons, inc.

Park, Y.J. and Ang, A.H.S. (1985), "Mechanistic seismic damage model for reinforced concrete", *J. Struct. Eng.*, ASCE, **111**(4), 722-739.

Patel, P.V., Raiyani, S.D. and Shah, P.J. (2018), "Torsional strengthening of RC beams using stainless steel wire mesh-Experimental and numerical study", *Struct. Eng. Mech.*, **67**(4), 391-401.

Rao, M.C., Bhattacharyya, S.K. and Barai, S.V. (2011), "Influence of field recycled coarse aggregate on properties of concrete", *Mater. Struct.*, **44**, 205-20.

Saleh, H.A., Al-Salloum, A.Y., Almusallam, T.H. and Nadeem, A.S. (2010), "Seismic response of FRP-upgraded exterior beam-column joints", *J. Compos. Constr.*, ASCE, **14**(2), 195-208.

Shaaban, I.G. and Seoud, O.A. (2018), "Experimental behavior of full-scale exterior beam-column space joints retrofitted by ferrocement layers under cyclic loading", *Case Stud. Constr. Mater.*, **6**, 61-78.

Shaikh, F., Kerai, S. and Kerai, S. (2015), "Effect of micro-silica on mechanical and durability properties of high volume fly ash recycled aggregate concretes (HVFA-RAC)", *Adv. Concrete Constr.*, **3**(4), 317-331.

Shannag, M.J. and Alhassan, M.A. (2005), "Seismic upgrade of interior beam-column sub-assemblages with high performance fiber reinforced concrete jackets", *ACI Struct. J.*, **102**(1), 131-138.

Silva, M.F.A. and Haach, V.G. (2016), "Parametrical study of the behavior of exterior unreinforced concrete beam-column joints through numerical modeling", *Comput. Concrete*, **18**(2), 215-233.

Subhash, C.Y., Dumpati, C.T. and Mohammed, S. (2016), "Performance studies on concrete with recycled coarse aggregates", *Adv. Concrete Constr.*, **4**(4), 263-281.

Teng, J.G., Chen, J.F., Smith, S.T. and Lam, L. (2002), *FRP-Strengthened RC Structures*, John Wiley & Sons, Ltd.

Tsonos, A.G. (2007), "Cyclic load behaviour of reinforced concrete beam-column subassemblages of modern structures", *ACI Struct. J.*, **194**(4), 468-478.

Tsonos, A.G. (2008), "Effectiveness of CFRP-jackets and RC-jackets in post-earthquake and pre-earthquake retrofitting of beam-column sub-assemblages", *Eng. Struct.*, **30**, 777-793.

Tsonos, A.G. (2009), "Ultra-high performance fiber reinforced concrete: an innovative solution for strengthening old R/C structures and for improving the FRP strengthening method", *Materials Characterization Computational Methods and Experiments IV*, WIT Transactions on Engineering Sciences, **64**, 273-284, The New Forest, UK.

Tsonos, A.G. (2014), "A new method for earthquake strengthening of old R/C structures without the use of conventional reinforcement", *Struct. Eng. Mech.*, **52**(2), 391-403.

Tsonos, A.G. (2014), "An innovative solution for strengthening of old R/C structures and for improving the FRP strengthening method", *Struct. Eng. Mech.*, **1**(3), 323-338.

Tsonos, A.G. and Papanikolaou, K.V. (2003), "Post-earthquake repair and strengthening of reinforced concrete beam-column connections (Theoretical and experimental investigation)", *Bull. NZ Soc. Earthq. Eng.*, **36**(2), 73-93.

Verma, S.K. and Ashish, D.K. (2017), "Mechanical behavior of concrete comprising successively recycled concrete aggregates", *Adv. Concrete Constr.*, **5**(4), 303-311.

Vidjeapriya, R. and Jaya, K.P. (2013), "Experimental study on two simple mechanical precast beam-column joints under reverse cyclic loading", *J. Perform. Constr. Facil.*, **27**(4), 402-414.

Viviana, C., Gonzalez, L. and Moriconi, G. (2014), "The influence of recycled concrete aggregates on the behavior of beam-column joints under cyclic loading", *Eng. Struct.*, **60**, 148-154.

Xiao, J., Sun, Y. and Falkner, H. (2006), "Seismic performance of frame structures with recycled aggregate concrete", *Eng. Struct.*, **28**, 1-8.

Xiao, J.Z., Li, W., Fan, Y. and Huang, X. (2012), "An overview of study on recycled aggregate concrete in China (1996-2011)", *Constr. Build. Mater.*, **31**, 364-83.

JK